https://doi.org/10.1016/j.proci.2022.08.024

H-abstractions by O_2, NO_2, NH_2, and HO_2 from H_2NO: theoretical study and implications for ammonia low-temperature kinetics

Alessandro Stagni*, Carlo Cavallotti

Department of Chemistry, Materials, and Chemical Engineering "G. Natta", Politecnico di Milano, Milano 20133, Italy

Abstract

Unraveling the low-temperature chemistry of ammonia is still an open challenge in combustion kinetics, yet of primary importance because of the novel combustion concepts operating in these conditions, as well as of the rising interest on ammonia as an energy carrier. In this work, a fundamental investigation of the H-abstraction reactions from H_2NO by O_2, NO_2, NH_2, and HO_2 was performed. These reactions, which belong to the radical-radical abstraction class, associate a high sensitivity to the key low temperature ammonia combustion parameters, to a high uncertainty in rate constant values. Theoretically, the investigation of reactions belonging to this class is complicated by their intrinsic multireference nature. To address this issue, a structured theoretical methodology that relies heavily on the use of CASPT2 calculations was devised. The predicted rate constants highlighted significant deviations from the rates commonly adopted in the state-of-the-art mechanisms, most often based on analogies and estimations. In order to understand their impact on ammonia low-temperature kinetics, the obtained rates were integrated into a kinetic model, which was used to investigate ammonia oxidation and ignition at low-temperature and oxygen-rich conditions. It was found that O_2 and NH_2 play the major role, as abstractors, in regulating ammonia oxidation and ignition. In particular, ignition delay time predictions proved extremely sensitive to the adopted rates: modifying each of them within their theoretical uncertainty caused deviations by even an order of magnitude, and totally changed the predictive features of the mechanism. The kinetic analysis highlighted then the need of a targeted optimization of the critical rates, downstream of the present work and within their uncertainty boundaries, to further refine the mechanism capability over a wide range of operating conditions.

Keywords: H_2NO; Ammonia; Low-temperature combustion; Ab initio; Chemical kinetics.

*Corresponding author.

1 Introduction

In the latest years, ammonia (NH_3) has become a key actor of the decarbonization process, due to its intrinsic carbon-free nature, its established production industry, and ultimately its physical properties, which make it an optimal e-fuel candidate to store the intermittent energy of renewable fuels [1]. Yet, there are major issues concerning the use of ammonia as an e-fuel related to its chemical features, such as low burning velocity and ignition delay times (IDTs), as well as formation of Nitrogen Oxides (NO_x) via the fuel mechanism [2]. In spite of this, since most of these limitations can be mitigated by blending ammonia with more reactive energy carriers, e.g. methane or hydrogen, unraveling its combustion chemistry has become a topical subject, both from an experimental and a theoretical point of view.

Such a research line actually started much earlier than the recent rise in the interest on ammonia. As a matter of fact, the understanding of its high-temperature pyrolysis mechanism is almost consolidated, with the first studies dating back to the 1980s [3–5]. On the other hand, research on its oxidation is relatively younger, and was first motivated by the use of ammonia in the context of the Thermal DeNO_x process for the selective, non-catalytic reduction of NO_x [6]. Above all, the massive introduction of theoretical chemistry for an *ab initio* evaluation of the elementary reaction steps [7] provided a significant acceleration to the fundamental research on nitrogen chemistry in combustion [2]. As a result, light has been shed on the different pathways involved in NO_x formation [8,9] and reduction [7], which were progressively included in the ammonia oxidation mechanisms released over the years [2,10–15].

To date, the most unclear aspects still needing to be addressed in ammonia combustion chemistry are its oxidation behavior at low-temperatures and when oxygen is abundant [2]. Such an operating range is indeed of particular interest for the most novel combustion concepts [16], as potentially able to ensure decreased pollutants emissions. From a chemical point of view, these conditions exhibit two major peculiarities: i) the presence of the HO_2 radical in considerable amounts due to its relative stability, so that the NH_2+HO_2 channel becomes critical [17–19]; ii) the formation in significant concentrations of nitroxide (H_2NO), i.e. one of the key compounds driving ammonia low-temperature oxidation. The contribution of this last species to the NH_3 oxidation mechanism has been assessed by several authors [2,16,19,20], who highlighted the high sensitivity of the low-temperature predictions on the reactions involving its formation and consumption. All of them pointed out the lack of experimental and theoretical information about H_2NO consumption via the related H-abstractions. To the authors' knowledge, the only theoretical evaluation was performed by Song et al. [22] with regard to H-abstraction by O_2, which was then adopted by Glarborg et al. [2] for kinetic modeling using a lowered activation energy. For the remaining abstractors, most of the adopted constants are indeed based on estimations [23,24].

In this context, this work provides a comprehensive theoretical investigation on H-abstractions from H_2NO, identified in the literature review as the most sensitive, as well as uncertain, steps in determining NH_3 reactivity at low-temperature and oxygen-rich conditions. The investigated reactions were:

$$H_2NO + HO_2 \rightarrow HNO + H_2O_2 \quad (R1)$$

$$H_2NO + NO_2 \rightarrow HNO + HONO \quad (R2)$$

$$H_2NO + O_2 \rightarrow HNO + HO_2 \quad (R3)$$

$$H_2NO + NH_2 \rightarrow HNO + NH_3 \quad (R4)$$

The theoretical determination of the rate constants for these reactions, which belong to the radical-radical abstraction class, is indeed particularly challenging [25]. The main reason lies in the electronic state changing significantly between reactants and products: from triplet (quadruplet for R3), to singlet (doublet for R3). The transition state (TS) has thus a marked multireference character, so that single reference methods routinely adopted to determine TS energies, gradients, and Hessians do not provide the proper theoretical context, and alternative electronic structure theories must be chosen. In the present work, in addition to determining rate constants of the mentioned reactions, a theoretical protocol that can be applied systematically to the investigation of the radical-radical abstraction reaction class was set up.

The calculated rates are finally adopted in the context of a detailed kinetic model to understand their importance in the critical operating space, as well as to understand couplings and competitions with the other sensitive reaction steps. Finally, conclusions and indications for future theoretical and kinetic-modeling research are provided.

2 Methodology

2.1 Theoretical methodologies

Rate constants for the four radical-radical abstraction reactions investigated in this work were determined using the *ab initio* transition state theory-based master equation (AITSTME) methodology. Specifically, the three-TS model implemented in EStokTP for abstraction reactions [26] was adopted. In this model the phenomenological rate constant is determined by solving the one dimensional master equation (ME) over a potential energy surface (PES) that contains two wells and three TSs. The two wells are the entrance and exit van der Waals (vdW) wells, which are connected to reactant and products through two TSs (outer TSs) and among themselves by the third TS (inner TS). The determination of rate constants through the integration of a ME for

abstraction reactions, for which intermolecular collisional energy transfer does not play any role, unless at low temperatures, is motivated by two reasons. First, it is useful as it allows to properly determine energy barriers to compute quantum tunneling corrections, for which the Eckart model was adopted. Secondly, and most importantly, it is necessary when the energy barrier of the inner TS is submerged, as it allows to properly cut the microcanonical reactive flux to the reactant asymptotic energy. The direct application of the macrocanonical formulation of conventional transition state theory through the computation of partition functions for TS and reactants would in fact lead to an overestimation of the reactive flux, and eventually of the rate constant.

Rate constants for the outer TSs were determined using phase space theory (PST) when the energy of the inner TS was positive, or only slightly submerged with respect to reactants. In these cases, the reactive flux is controlled by the inner TS, and uncertainties in PST do not affect the rate constant value. Phase space theory was implemented using an attractive $1/R[Bohr]^6$ potential and a standard pre-factor of 10 au. The van der Waals wells contribution is relevant only for HO_2 abstraction at 500 K and below for pressures higher than 10 bar. For reaction R4, where the barrier is significantly submerged, the rate of the entrance channel was determined using Variable Reaction Coordinate Transition State Theory (VRC-TST). VRC-TST calculations, whose purpose is thus that of determining the rate of formation of the entrance van der Waals well, were performed using two pivot points, located on the centers of mass of the two fragments, computing energies at the CASPT2/cc-pVDZ level using a minimal (2e,2o) active space. According to past experience [27], the correction potential in the region of transition between long range and short range dividing surfaces, thus where the long range interaction potential is maximum, is often small for CASPT2(2e,2o)/cc-pVDZ energies. The rate constants of inner TSs were determined using conventional TST in the rigid rotor harmonic oscillator approximation (RRHO), substituting low vibrational frequencies representative of internal torsional motions with 1D hindered rotor models. For this purpose, the selected torsional motions were projected out of the Hessian using the procedure implemented in EStokTP. The H_2NO radical has some peculiar features. Its atomic arrangement is slightly non planar, with an out-of-plane umbrella motion that is highly anharmonic. Following the study of Song et al. [22], who found out that at combustion temperatures the thermal energy is sufficient to overcome the umbrella inversion barrier, we computed its density of states using a rotational symmetry number of 2 and a harmonic oscillator model with a frequency of 449 cm^{-1}, which allowed reproducing the same partition function (with a maximum 10% error between 300 K and 2000 K) calculated with the eigenvalues determined by Song et al. using a 1D umbrella inversion quantum model [22]. Structures, Hessians, and energies of reactants, products, vdW wells, and TSs were determined at two levels of theory. At both levels it was assumed that reactions take place on PESs accessed upon spin pairing of the reacting radicals, thus on the singlet PES when the reactants are doublet radicals, and on the doublet PES when one reactant is a doublet and the other a triplet (i.e. for H_2NO+O_2). On the singlet PES, the system behaves as a diradical up to the transition state, in proximity of which the spin paired singly occupied radical orbitals combine into one molecular orbital.

Some test calculations showed that reactions proceeding on higher spin PESs have higher energy barriers, and are therefore not competitive. At the first level of theory structures and Hessians were determined at the ωB97X-D/jun-cc-pVTZ level. All TSs and vdW wells simulations were performed using unrestricted wave functions and broken symmetry guesses. High level energies (E(HL)) were computed at the CCSD(T) level extrapolating to the complete basis set limit (CBS) using the density fitted (DF) formalism at the MP2 level and accounting for corrections for core electrons excitations as:

$$E(HL)=E(CCSD(T)/aug\text{-}cc\text{-}pVTZ)+ [E(CCSD(T,core)/cc\text{-}pVTZ)- E(CCSD(T)/cc\text{-}pVTZ)] +[E(DF\text{-}MP2/CBS)- E(DF\text{-}MP2/aug\text{-}cc\text{-}pVTZ)] \quad (1)$$

where E(MP2/CBS) is defined as:

$$E(DF\text{-}MP2/CBS)=E(DF\text{-}MP2/aug\text{-}cc\text{-}pVTZ)] +0.58[E(DF\text{-}MP2/aug\text{-}cc\text{-}pVQZ) -E(DF\text{-}MP2/aug\text{-}cc\text{-}pVTZ)] \quad (2)$$

The E(MP2/CBS) extrapolation was performed using Martin's two parameter scheme [28]. As will be shown in the result section, this approach allows determining 0K reaction enthalpy changes (ΔH(0K)) within chemical accuracy for all investigated reactions. However, all TSs determined at this level of theory have large T1 diagnostics, which is indicative of a significant multireference character and motivated the use of a different theoretical protocol.

At the second level of theory, structures and Hessians of TSs, reactants, and products were determined at the CASPT2/aug-cc-pVTZ level. Calculations were performed using the largest active spaces (AS) computationally feasible, in which all the orbitals that change significantly between reactants and TS were included, with the intent to obtain a balanced AS. As test calculations showed, this system is significantly affected by the presence of intruder states, which could be removed only using an IPEA shift of 0.25. Energies were determined using two methods on CASPT2 optimized structures. In the first method energies were computed with respect to those of reactants (or products), whose structure was optimized at fixed separations (10 Å) at the same level as the TS, using AS systematically increased up to the maximum size that is computationally feasible.

Unfortunately, it was not possible to reach the full valence space, which would be the ideal AS for multireference calculations, for any of the investigated systems. The reference species (reactants or products) chosen for the evaluation of the relative energy were those on the endothermic side of the reaction, thus those for which the energy difference with respect to the TS is minimal. This allowed minimizing the error in the computational procedure. As in some cases it was found that the energies calculated with this methodology are quite sensitive to the adopted AS, they were estimated using a second methodology. In fact, as noted recently by Klippenstein and co-workers [19], multireference methodologies are more accurate in determining energy differences between different spin states rather than relative energy changes between stationary points on the same PES. On the other side, PESs with higher spin multiplicity than those of the TS can be described reasonably well using single-reference methods, so that the energy of the TS can be efficiently determined on CASPT2 structures as: the sum between the E(HL) energy difference between reactants and TS computed on the higher spin PES and of the energy change from the higher to the lower spin PES computed at the CASPT2 level.

CCSD(T), CASPT2, and DF-MP2 calculations were performed with MOLPRO 2021 [29], while ωB97X-D calculations with Gaussian 09 [30]. Master equations simulations were performed with MESS [31]. Transition states, frequency projections, and ME inputs assembly were performed using EStokTP [26].

2.2 Kinetic modeling

The kinetic model describing NH_3 pyrolysis and oxidation was set up starting from the previous work of Stagni et al. [17], where it was developed by following a first-principles approach; here, the latest available kinetic rates for ammonia pyrolysis and oxidation as well as NO_x formation, were combined to a theoretical reassessment of a subset of specific reactions, identified on the basis of sensitivity analysis and a literature review of their uncertainty range. Specifically, they were: i) NH_3 and HNO decomposition; ii) H-abstraction from NH_3 by H, OH, O, O_2, and HO_2. The remaining part of the mechanism included a core H_2/O_2 mechanism, taken from the work of Metcalfe et al. [32], while the subset of NO_x reactions was adopted after the work of Song et al. [33]. Thermal DeNO_x reactions (NH_2+NO), as well as the corresponding reactions involving NO_2 (NH_2+NO_2), were assigned the values suggested by Glarborg et al. in their recent review [2].

The two major changes performed on the Stagni framework involved i) the H-abstractions from H_2NO by O_2, NO_2, NH_2 and HO_2 as calculated in this work, and ii) the kinetic rates and branching fractions (BF) of the NH_2+HO_2 reaction, recently recalculated by Klippenstein and Glarborg, along with the H-abstraction from H_2NO by OH [19]. As a result, the H-abstraction from NH_3 by O_2 calculated in [17] was replaced by its reverse rate (but were within a factor ~1.2 for T > 500 K), while the channel providing H_2NO+OH, previously adopting the low-temperature rate proposed by Baulch et al. [34], was replaced by the newer evaluation [19]. In this case, while being comparable at 300 K, the new rate was lower by a factor ~3 at 1000 K.

The updated mechanism was used in this work for a first quantification of the role of the updated reaction rates in the NH_3 low-temperature chemistry, as well as the effect of their uncertainty on the modeling predictions. It is available in the SM in CHEMKIN format, together with thermodynamic and transport properties.

3 Results and discussion

3.1 Potential Energy Surface

Enthalpy changes, calculated at 0 K using the first level of theory used in the present study, are compared to experimental data in Table 1. As can be noticed, the theoretical predictions are well within chemical accuracy (1 kcal/mol), being 0.4 kcal/mol the maximum difference between experimental and calculated data. All reactions are exothermic, except the H-abstraction by oxygen, which is endothermic by about 13 kcal/mol.

Table 1
Enthalpy changes (kcal/mol) for H abstraction reactions from HNO_2 computed at 0 K at level of theory 1 (single reference), as defined in the text, compared with ATCT [35] experimental data. ZPE corrections are included.

Reaction	ΔH(0K)	ATCT
$H_2NO+HO_2 \rightarrow HNO+H_2O_2$	-24.8	-25.2
$H_2NO+NO_2 \rightarrow HNO+HONO$	-16.7	-16.9
$H_2NO+O_2 \rightarrow HNO+HO_2$	13.2	12.9
$H_2NO+NH_2 \rightarrow HNO+NH_3$	-44.7	-45.0

Structures of TSs were initially determined using EStokTP automated procedures, which include also a scan around torsional bonds to search for the minimum energy saddle point. Energy barriers, calculated at the first level of theory used in this study, thus through equation (1) with ZPE corrections determined at the ωB97X-D/jun-cc-pVTZ level, are reported in Table 2 together with the relative CCSD(T)/aug-cc-pVTZ T1 diagnostics.

As can be noticed, the T1 diagnostics are particularly high for a closed shell system, where a value higher than 0.02 is usually indicative of significant multireference character. This is however only partially true for H-abstraction by O_2, which occurs on the open shell doublet PES, in which case T1 diagnostics of 0.035 are often considered as acceptable. Its energy barrier is in good agreement with the 23.2 kcal/mol computed by Song et al. [22]

using QCISD(T)/6-311G(d,p) structures and CCSD(T) energies extrapolated to the CBS.

Table 2
Energy barriers (kcal/mol) for H-abstraction reactions from H_2NO computed at 0 K at level of theory 1 (single reference), as defined in the text, and relative T1 diagnostics. ZPE corrections are included.

Reaction	$E^{\ddagger}$	T1
$H_2NO+HO_2 \rightarrow HNO+H_2O_2$	-1.3	0.043
$H_2NO+NO_2 \rightarrow HNO+HONO$	0.2	0.031
$H_2NO+O_2 \rightarrow HNO+HO_2$	23.1	0.037
$H_2NO+NH_2 \rightarrow HNO+NH_3$	-3.1	0.043

Structures of TSs were then determined at the CASPT2 level of theory. A significant difference was observed with respect to structures determined at the ωB97X-D level, so that using the latter structures as guesses for geometry optimization did not systematically allow to obtain converged results. The structures of the TSs determined for H-abstraction by O_2 are compared in Figure 1. The H-O distance increases in the CASPT2 structure from 1.32 Å to 1.39 Å, while the H-O distance decreases from 1.15 Å to 1.11 Å, thus indicating that the in multireference structure the TS is looser, or that it occurs earlier (looking at the reaction from the endothermic side, i.e. $HNO+ HO_2 \rightarrow H_2NO+O_2$). A feature that is markedly different between the two TSs is the establishment of an intermolecular interaction between the O atoms of the reactants, which is more significant in the CASPT2 structure, with a distance of 2.31 Å, than in the single reference ωB97X-D structure. Similar differences between single reference and multireference structures have been observed also for the other TSs. The energy barriers calculated at the

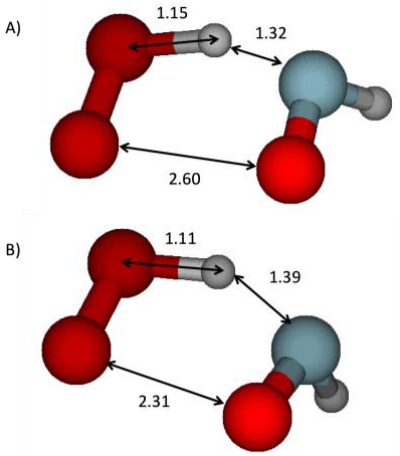

Figure 1. TS structures for the H_2NO+O_2 reaction computed at the ωB97X-D/jun-cc-pVTZ and CASPT2(13e,10o)/aug-cc-pVTZ levels. Distances are reported in Angstroms.

Table 3
Energy barriers (kcal/mol) for H-abstraction reactions from HNO_2 computed at 0 K at level of theory 2 (multireference), as defined in the text, using two approaches: A) at the CASPT2 level with respect to reactants; B) triplet-singlet gap at the CASPT2 level and HL energy difference with respect to reactants on the triplet PES as defined by equation 1, except for H_2NO+O_2 (see note b). ZPE corrections are included.

	$E^{\ddagger}$	
Reaction	A	B
$H_2NO+HO_2 \rightarrow HNO+H_2O_2$	-3.9[b]	-2.8
$H_2NO+NO_2 \rightarrow HNO+HONO$	2.8	-1.4[b]
$H_2NO+O_2 \rightarrow HNO+HO_2$	19.3[b]	19.8[a]
$H_2NO+NH_2 \rightarrow HNO+NH_3$	-8.7[b]	-8.0

a) Doublet-quadruplet energy gap and HL on the quadruplet PES; b) used to compute rate constant.

multireference level using the two methodologies described in the method section are reported in Table 3. Details of the active spaces used in the simulations are reported as SM in Table S1. It can be noted that the energy barriers computed at the two different levels of theory are consistent within 1 kcal/mol, except for NO_2 abstraction. In this case the energy barrier was computed using method B, as the systematic increase of the AS for the determination of the energy barrier was still showing significant fluctuations when the highest size that is computationally feasible was reached, i.e. (16e,12o). Indeed, it was found that increasing the active space from (14e,10o) to (16e,12o) led to a decrease of the energy barrier from 4.1 to 2.8 kcal/mol, thus indicating that the AS is not well balanced. It should be noted that this is not a problem for the calculation of the singlet-triplet energy gap, which is less sensitive to the AS size. Rate constants were therefore determined using the -1.4 kcal/mol energy barrier computed using method B. The comparison of the energy barriers reported in Table 3 with those of Table 2 evidences remarkable differences. The multireference energy barriers are between 1.6 and 5.6 kcal/mol smaller than those determined with single reference methods. This indicates that standard single-reference approaches used for determining rate constants for abstraction reactions can lead to considerable errors when used for radical-radical abstractions for which products and reactants have different spin multiplicities. It can be noted that the difference in energy barrier computed by Song et al. [22] and the present work using a single reference approach and the one determined using the multireference approach for H_2NO+O_2 is large: 3.8 kcal/mol. As this reaction plays an important role in determining ammonia oxidation kinetics at low temperatures, it is interesting to notice that Glarborg et al. [2] reduced the activation energy of the rate constant computed by Song [22] by 2.4 kcal/mol, i.e. to a value close to the one here computed, in order to

better fit the experimental data concerning NH_3 oxidation and thermal $DeNO_x$ with high oxygen amounts.

3.2 Alternative reaction pathways

In the present work, the focus on the analysis has been on radical-radical H-abstraction of H_2NO hydrogen atoms by several radicals. However, it is possible that other reaction pathways involving the same radicals but entering the reactive PES through an addition step may be competitive. To investigate whether this is the case for the reaction with OOH the H_2NO+OOH reaction proceeding through the formation of the H_2NOOOH adduct was studied at the ωB97X-D/jun-cc-pVTZ level of theory. The calculations showed that this adduct decomposes to $HNO+H_2O_2$ through the same TS that is reached without preliminary addition, as the H_2NO-OOH bond is weak (2 kcal/mol) and breaks along the reaction path. The competitive H_2NOOOH decomposition pathway leading to $H_2NOO+OH$ is endothermic by 28 kcal/mol (with respect to the H_2NOOOH adduct), which makes it unfavored with respect to the H-abstraction route.
The $H_2NO+OOH \rightarrow H_2NOH+OO$ reaction pathway was also investigated. Its rate constant, determined at the highest single reference level of theory used in this work, is between a factor of 5 and 10 smaller than that for direct abstraction, depending on the temperature. Finally, the $H_2NO+NH_2 \rightarrow H_2NOH+NH$ reaction is endothermic by 68 kcal/mol, thus not competitive with the abstraction channel.

3.3 Evaluation of rate constants

Rate constants for reactions R1-R4, computed integrating the ME as described in section 2.1, were fitted in the modified Arrhenius form as reported in Table 4. As a representative example, the rate constant for H-abstraction by O_2 is compared with the literature estimation by Song et al. [22] and Glarborg et al. [2] in Figure 2. At 1000 K, the evaluated rate is 4.5 times faster than what calculated by Song et al. [22]. On the other hand, the rate is in agreement with the value adopted by Glarborg et al. [2], who modified Song value to improve modeling predictions. Such

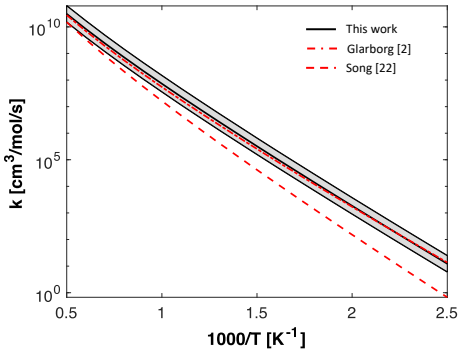

Figure 2. Rate constant calculated for H-abstraction from H_2NO by O_2, compared to literature [2,19]. The shaded area represents a factor 2 deviation from the proposed rate.

modification brought the rate constant within a factor 2 from the rate calculated in this work, which is well within the uncertainty of the present calculations (about 1 kcal/mol in energy barrier and a factor of 1.5 in the pre-exponential factor, because of anharmonicities and the relatively low quality of CASPT2 vibrational frequencies, thus around a factor of 2 on average). Comparisons with the available literature data concerning the remaining rates are provided in the SM.

Table 4
Rate constants for H-abstraction reactions from H_2NO computed solving the three TSs ME and fitted to the modified Arrhenius form as $k = AT^{\alpha}\exp[-E_{act}/(RT)]$. Units are cm, cal, mol, K

Reaction	A	α	E_{act}
$H_2NO+HO_2 \rightarrow HNO+H_2O_2$	5.41e4	2.16	-3597
$H_2NO+NO_2 \rightarrow HNO+HONO$	7.95	2.95	-3293
$H_2NO+O_2 \rightarrow HNO+HO_2$	1.73e5	2.19	18010
$H_2NO+NH_2 \rightarrow HNO+NH_3$	9.49e12	-0.08	-1644

3.4 Implications for ammonia low-temperature chemistry

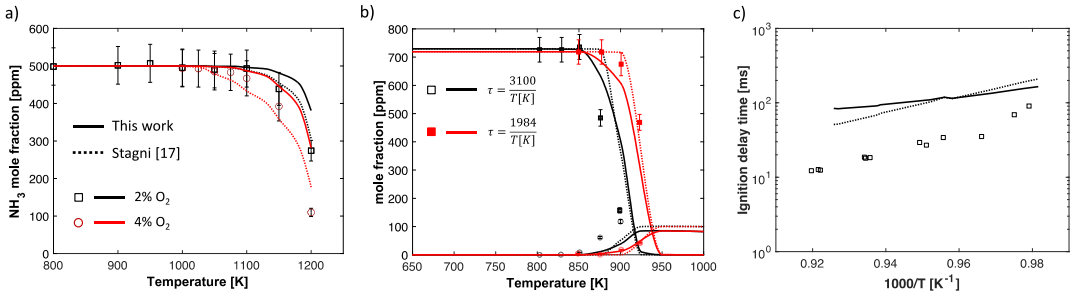

Figure 3. a) NH_3 oxidation in a Jet Stirred reactor. P = 800 torr. τ = 1.5 s [14]. b) NH_3 oxidation in a Flow reactor. Φ = 0.22. P = 30 bar. [19] c) Ignition delay time in a Rapid Compression Machine (RCM). Φ = 0.35. P_c = 43.4 bar [17]. $X_{NH_3} = 8.93\%$, $X_{O_2} = 19.13\%$, $X_{N_2} = 61.15\%$, $X_{Ar} = 10.79\%$.

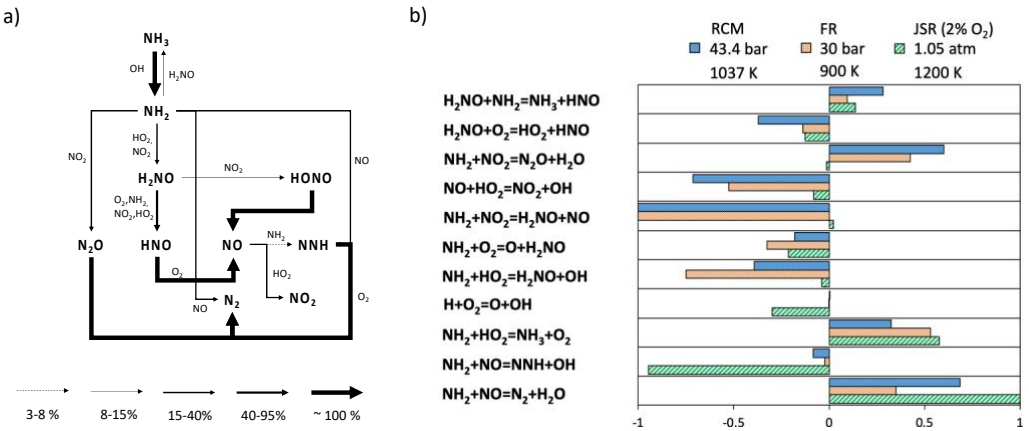

Figure 4. a) Reaction Flux analysis for NH_3 oxidation in a flow reactor at T = 900 K and P.= 30 bar, (cfr. Figure 3b) at a reactor length corresponding to 1% fuel conversion. b) Sensitivity analysis to NH_3 mass fraction (at 1% NH_3 conversion, for RCM and FR).

Low-temperature chemistry datasets on ammonia oxidation have been collected in a wide range of devices and operating conditions. Figure 3 provides an overview of the numerical predictions of the kinetic model implementing the calculated H-abstractions from H_2NO, as well as the recent rates and BFs of the NH_2+HO_2 channel. For the sake of completeness, the predictions provided by the starting model by Stagni et al. [17] are reported as well. Simulations were performed via the OpenSMOKE++ framework [36].

Three different pressure levels are considered, in lean or very lean conditions, so as to emphasize oxidation conditions. Compared to the starting model, at near-atmospheric pressure (Figure 3a) the reactivity is delayed by ~30 K and ~50 K, respectively, for O_2 = 2% and 4%, such that the reactivity onset is at the upper limit of the experimental uncertainty. At P = 30 bar (flow reactor – Figure 3b [22]), the updated model provides a better description of the NH_3 consumption rate with the temperature for both residence times, and only a shift of 10-15 K is present in predicting the conversion temperatures. Finally, in terms of low-temperature ignition delay times at high pressures (Figure 3c [20]), the updated model provides a worsened slope over the temperature range, although improvements are observed, in absolute terms, at the lowest temperatures.

In order to shed light on the role played by H_2NO in this range of conditions, Figure 4 shows a flux analysis in sample conditions, and a sensitivity analysis to NH_3 mass fraction in all of the three reactors considered. The key role played by H_2NO is apparent in the reaction flux: after NH_2 is generated, ammonia conversion to NO and N_2 can proceed via three alternative paths: i) via NO (thermal $DeNO_x$), ii) via NO_2, or iii) via HO_2. Each of these pathways has a propagation and a termination channel.

The formation of H_2NO via NO_2 or HO_2 boosts ammonia oxidation, since it can be abstracted to HNO, and finally to NO. In this pathway, H-abstraction by O_2 enhances the reactivity, since it provides a HO_2 radical, on turn converted to OH via the NH_2+HO_2 propagation channel. On the other hand, the remaining H-abstractions are antagonist to this process, since they return more stable products (NH_3, H_2O_2, HONO). This is confirmed by the sensitivity analysis performed at the different conditions (Figure 4b). At near-atmospheric pressure, thermal $DeNO_x$ drives the oxidation process due to the higher presence of NO compared to NO_2. Here, the H-abstraction from H_2NO by NH_2 is one of the main inhibithors of the oxidation process. The higher rate compared to the work used in [17] (cfr. Figure S3) justifies the overall slower oxidation rate. When increasing the pressure, the pathways via NO_2 and HO_2 become determining, so that the competition between the related propagation and termination channels controls NH_3 oxidation.

In all the investigated cases, 2 out of the 4 H-abstractions calculated in this work affect the final reactivity to a major extent, and involve O_2 (R3) and

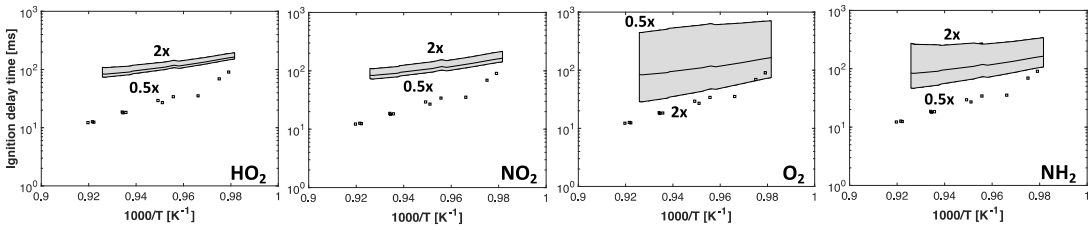

Figure 5. Brute-force sensitivity analysis to ignition delay time in RCM (cfr Figure 3c) [17], by varying R1 to R4 by a factor 2.

NH_2 (R4) as abstractors (in opposite directions). The remaining 2 abstractors considered in this work play instead a much more important role in reacting with NH_2.

Finally, sensitivity analysis shows that the importance of the investigated H-abstractions is maximum in driving NH_3 ignition delay times: in order to quantify such effect in macroscopic terms, Figure 5 shows a brute-force sensitivity analysis for all of investigated H-abstractions: for the case analyzed in Figure 3c, the pre-exponential factor of each reaction was separately varied by a factor 2, i.e. still within their uncertainty limits, and the IDT recalculated. Results confirm the key importance of R3 and R4: for R3, more than an order of magnitude is present between the upper and lower boundaries, whilst being slightly lower than a factor of 10 for R4. Considering that at such pressures, IDTs also depend on the total NH_2+HO_2 and NH_2+NO_2 rate constants, as well as the respective branching between propagation and termination channels, the unavoidable associated uncertainties suggest to extend the perspective towards kinetic modeling and optimization, downstream of the theoretical framework provided in this work.

4 Conclusions

In this work, a theoretical quantification of the rate constants of the key H-abstractions from H_2NO, of critical relevance for the low-temperature oxidation of ammonia, was performed by adopting the *ab initio* transition state theory-based master equation methodology. Because of the significant difference between the electronic structure of reactants and products, a computation protocol for the evaluation of radical-radical abstraction reactions was set up, and systematically applied considering HO_2, NO_2, O_2, and NH_2 as target abstractors.

Comparing the obtained rates to literature data highlighted several differences with respect to the kinetic rates available in the state-of-the-art NH_3 mechanisms, where the only theoretical value used so far was H-abstraction by O_2 [22], while the remaining ones were mostly based on estimations or analogies.

Implementing the kinetic rates within a recent ammonia mechanism [17] allowed to frame their role in a wide range of operating conditions. The kinetic analysis of three case studies at low temperature and variable pressures allowed to identify the key role of NH_2 and O_2 as abstractors, affecting both speciation and ignition delay time. Although their effect on the reactivity is overlapped with NH_2+NO, NH_2+NO_2 and NH_2+HO_2 product channels, they turned out to be particularly critical in controlling ignition delay times at high pressures. In this case, varying them within their uncertainty boundaries resulted in a change in predictions up to an order of magnitude. Therefore, although this work provided a consolidated theoretical foundation for these key reactions, a downstream kinetic modeling and optimization step is still needed, in order to reconcile the modeling predictions with the vast amount of available experimental data.

Supplementary material

Supplementary material associated with this article, can be found, in the online version, at doi:YYY

References

[1] H. Kobayashi, A. Hayakawa, K.D.K.A. Somarathne, E.C. Okafor, Science and technology of ammonia combustion, *Proc. Combust. Inst.* 37 (2019) 109–133.

[2] P. Glarborg, J.A. Miller, B. Ruscic, S.J. Klippenstein, Modeling nitrogen chemistry in combustion, *Prog. Energy Combust. Sci.* 67 (2018) 31–68.

[3] J. V. Michael, J.W. Sutherland, R.B. Klemm, The flash photolysis—shock tube technique using atomic resonance absorption for kinetic studies at high temperatures, *Int. J. Chem. Kinet.* 17 (1985) 315–326.

[4] D.F. Davidson, K. Kohse-Höinghaus, A.Y. Chang, R.K. Hanson, A pyrolysis mechanism for ammonia, *Int. J. Chem. Kinet.* 22 (1990) 513–535.

[5] J.A. Miller, C.T. Bowman, Mechanism and modeling of nitrogen chemistry in combustion, *Prog. Energy Combust. Sci.* 15 (1989) 287–338.

[6] R.K. Lyon, Thermal DeNOx Controlling nitrogen oxides emissions by a noncatalytic process, *Environ. Sci. Technol.* 21 (1987) 231–236.

[7] S.J. Klippenstein, From theoretical reaction dynamics to chemical modeling of combustion, *Proc. Combust. Inst.* 36 (2017) 77–111.

[8] S.J. Klippenstein, L.B. Harding, B. Ruscic, et al., Thermal decomposition of NH2OH and subsequent reactions: Ab initio transition state theory and reflected shock tube experiments, *J. Phys. Chem. A.* 113 (2009) 10241–10259.

[9] S.J. Klippenstein, L.B. Harding, P. Glarborg, J.A. Miller, The role of NNH in NO formation and control, *Combust. Flame*. 158 (2011) 774–789.

[10] O. Mathieu, E.L. Petersen, Experimental and modeling study on the high-temperature oxidation of Ammonia and related NOx chemistry, *Combust. Flame*. 162 (2015) 554–570.

[11] K.P. Shrestha, L. Seidel, T. Zeuch, F. Mauss, Detailed Kinetic Mechanism for the Oxidation of Ammonia Including the Formation and Reduction of Nitrogen Oxides, *Energy and Fuels*. 32 (2018) 10202–10217.

[12] R. Li, A.A. Konnov, G. He, F. Qin, D. Zhang, Chemical mechanism development and reduction for combustion of NH3/H2/CH4 mixtures, *Fuel*. 257 (2019) 116059.

[13] X. Zhang, S.P. Moosakutty, R.P. Rajan, M. Younes, S.M. Sarathy, Combustion chemistry of ammonia/hydrogen mixtures: Jet-stirred reactor measurements and comprehensive kinetic modeling, *Combust. Flame*. 234 (2021) 111653.

[14] B. Mei, J. Zhang, X. Shi, Z. Xi, Y. Li, Enhancement of ammonia combustion with partial fuel cracking strategy: Laminar flame propagation and kinetic

modeling investigation of NH3/H2/N2/air mixtures up to 10 atm, *Combust. Flame*. 231 (2021) 111472.
[15] S.A. Alturaifi, O. Mathieu, E.L. Petersen, An experimental and modeling study of ammonia pyrolysis, *Combust. Flame*. 235 (2022) 111694.
[16] A. Cavaliere, M. De Joannon, Mild combustion, *Prog. Energy Combust. Sci.* 30 (2004) 329–366.
[17] A. Stagni, C. Cavallotti, S. Arunthanayothin, et al., An experimental, theoretical and kinetic-modeling study of the gas-phase oxidation of ammonia, *React. Chem. Eng.* 5 (2020) 696–711.
[18] P. Glarborg, H. Hashemi, S. Cheskis, A.W. Jasper, On the Rate Constant for NH2+ HO2 and Third-Body Collision Efficiencies for NH2+ H (+ M) and NH2+ NH2 (+ M), *J. Phys. Chem. A*. 125 (2021) 1505–1516.
[19] S.J. Klippenstein, P. Glarborg, Theoretical kinetics predictions for NH2+ HO2, *Combust. Flame*. 236 (2022) 111787.
[20] M. Pochet, V. Dias, B. Moreau, et al., Experimental and numerical study, under LTC conditions, of ammonia ignition delay with and without hydrogen addition, *Proc. Combust. Inst.* 37 (2019) 621–629.
[21] X. He, B. Shu, D. Nascimento, et al., Auto-ignition kinetics of ammonia and ammonia/hydrogen mixtures at intermediate temperatures and high pressures, *Combust. Flame*. (2019).
[22] Y. Song, H. Hashemi, J.M. Christensen, et al., Ammonia oxidation at high pressure and intermediate temperatures, *Fuel*. 181 (2016) 358–365.
[23] P. Glarborg, K. Dam-Johansen, J.A. Miller, R.J. Kee, M.E. Coltrin, Modeling the thermal DENOx process in flow reactors. Surface effects and nitrous oxide formation, *Int. J. Chem. Kinet.* 26 (1994) 421–436.
[24] A.M. Dean, J.W. Bozzelli, Combustion Chemistry of Nitrogen, in: Gas-Phase Combust. Chem., 2000: pp. 125–341.
[25] S.J. Klippenstein, C. Cavallotti, Ab initio kinetics for pyrolysis and combustion systems, in: Comput. Aided Chem. Eng., Elsevier B.V., 2019: pp. 115–167.
[26] C. Cavallotti, M. Pelucchi, Y. Georgievskii, S.J. Klippenstein, EStokTP: Electronic Structure to Temperature- and Pressure-Dependent Rate Constants—A Code for Automatically Predicting the Thermal Kinetics of Reactions, *J. Chem. Theory Comput.* 15 (2019) 1122–1145.
[27] J. Lupi, C. Puzzarini, C. Cavallotti, V. Barone, State-of-the-art quantum chemistry meets variable reaction coordinate transition state theory to solve the puzzling case of the H2S+ Cl system, *J. Chem. Theory Comput.* 16 (2020) 5090–5104.
[28] J.M.L. Martin, Ab initio total atomization energies of small molecules — towards the basis set limit, *Chem. Phys. Lett.* 259 (1996) 669–678.
[29] H.-J. Werner, P.J. Knowles, F.R. Manby, et al., The Molpro quantum chemistry package, *J. Chem. Phys.* 152 (2020) 144107.
[30] M.J. Frisch, G.W. Trucks, H.B. Schlegel, et al., Gaussian 09, Rev. D.01, *Gaussian Inc., Wallingford, CT*. (2016).
[31] Y. Georgievskii, J.A. Miller, M.P. Burke, S.J. Klippenstein, Reformulation and solution of the master equation for multiple-well chemical reactions, *J. Phys. Chem. A*. 117 (2013) 12146–12154.
[32] W.K. Metcalfe, S.M. Burke, S.S. Ahmed, H.J. Curran, A hierarchical and comparative kinetic modeling study of C1 - C2 hydrocarbon and oxygenated fuels, *Int. J. Chem. Kinet.* 45 (2013) 638–675.
[33] Y. Song, L. Marrodán, N. Vin, et al., The sensitizing effects of NO2 and NO on methane low temperature oxidation in a jet stirred reactor, *Proc. Combust. Inst.* 37 (2019) 667–675.
[34] D.L. Baulch, C.T. Bowman, C.J. Cobos, et al., Evaluated kinetic data for combustion modeling: supplement II, *J. Phys. Chem. Ref. Data*. 34 (2005) 757–1397.
[35] B. Ruscic, D.H. Bross, Active Thermochemical Tables (ATcT) values based on ver. 1.122d of the Thermochemical Network, 2018.
[36] A. Cuoci, A. Frassoldati, T. Faravelli, E. Ranzi, OpenSMOKE++: An object-oriented framework for the numerical modeling of reactive systems with detailed kinetic mechanisms, *Comput. Phys. Commun.* 192 (2015) 237–264.